Moroccan Journal of Chemistry
ISSN: 2351-812X
http://revues.imist.ma/?journal=morjchem&page=login
Abubakar & al. / Mor. J. Chem. 7 N°1(2019) 082-097

Investigation of Corrosion Inhibition potential of Ethanol Extract of *Balanites aegyptiaca* Leaves on Mild Steel in 1 M Hydrochloric Acid Solution.

M. S. Abubakar [(a)]* and B. Usman[(b)]

[(a)] Department of Pure and Industrial Chemistry, Faculty of Physical Science, College of Natural and Pharmaceutical Sciences, Bayero University, Kano, P.M.B 3011, Nigeria

** Corresponding author:*
abubakarshehumohammed1@gmail.com

Received 10 Jan 2019,
Revised 12 Feb 2019,
Accepted 21 March 2019

Abstract

The corrosion inhibition effect of *Balanites aegyptiaca* leaves extract (BALE) on mild steel in 1 M hydrochloric acid solution has been investigated using gravimetric study and potentiodynamic polarization (PDP) measurements. The inhibition efficiency from weight loss studies was found to be 96.64% whereas 99.98% was obtained from potentiodynamic polarization studies at optimum concentration of 1.25 g/L of BALE. The PDP studies revealed that the BALE at different concentrations of the inhibitor acted as a mixed-type inhibitor. The inhibition efficiency is found to increase with increase in concentrations of the inhibitor and decrease with rise in temperature. The thermodynamic parameters and results from UV (i.e shift of bands from 227.84nm to 223.84nm and appearance of 203.94nm, 207.99nm and 325nm) and FTIR (shift from 1208cm^{-1} to 1205 cm^{-1} and 1618 cm^{-1} to 1611 cm^{-1} and appearance of new 1016 cm^{-1}, 1676 cm^{-1}, 1834 cm^{-1}, 3905 cm^{-1} bands etc) revealed the adsorption of the inhibitor molecules on mild steel surface as comprehensive adsorption (physical and chemical adsorption) and closely obey Langmuir adsorption isotherm. Surface analysis by UV, FTIR, XRD and SEM confirmed the formation of the adsorbed layer on the mild steel surface.

Keywords: *Corrosion inhibition, mild steel, comprehensive adsorption, BALE, potentiodynamic polarization.*

1. Introduction

Mild steel is one of the most applicable constructional materials extensively used in widest range of industries where aggressive acid solutions are widely in application [1]. However, as observed by Lgaz *et al.*, 2017 and anupama *et al.*, 2016 [1] [2] more than a quarter of the world's steel production is degraded due to a corrosion problem. This problem therefore, necessitated the indispensable use of corrosion inhibitors in order to mitigate the attacks on metallic materials by the corrosive media. Unfortunately, the inhibitors mostly used are inorganic and synthetic in nature which have been proven to be very hazardous to human health causing cancerous diseases, exorbitant-cycle costing and are not environmentally friendly [3] [4]. In view of this development, the present research study investigated an economically viable and scalable source of green corrosion inhibitor (*Balanites aegyptiaca* leaves extract) which is biodegradable and environmentally friendly using gravimetric method and potentiodynamic polarization techniques. The source plant (*Balanites aegyptiaca*) is abundantly distributed across Africa, South Asia, Middle East, etc and also possesses potential health benefits but nevertheless unkempt [5] [6] [7].

2.0. Materials and Methods

2.1 Preparation of the metal coupons

The metal used for this study were mild steel sheets obtained from the Department of Mechanical Engineering, Bayero University, Kano with composition (wt %) Mn (0.27), Al (0.04), C (0.066), Ca (0.01), Cr (0.041), Cu (0.023), I (0.25), Te (0.17), Cl (0.25), Sc (0.03), Sb (0.24), Eu (0.10), Si (0.13) and Fe (98.42) and dimension of 2cm x 2cm x 0.1cm.

2.2 Preparation of the inhibitor

The ethanol was the solvent used for the extraction of *Balanites aegyptiaca* leaves extract. All the reagents used in this study were of analytical grade reagent. The sample leaves of *Balanites aegyptiaca* were obtained from Tirwun District of Bauchi Local Government Area, Bauchi State, Nigeria. The leaves samples were washed and shade dried for 21 days and ground to fine powder. 250 g of leaves powder were extracted using Soxhlet extractor for 40 hr loading 50 g/800 cm^3 of the ethanol at a time. The solution was evaporated using a Rotary evaporator, Model R-210, at 48^oC to obtain the concentrated crude extract. The crude extract was dried, stored in a clean bottle and covered properly [4].

2.3 Preparation of the Test Media

The aggressive test media of 1 M HCl acid stock solution was prepared using analytical-grade 37% of HCl with double distilled water. The concentration of the inhibitors ranging from (0.25-1.25)g/L were then prepared for this study.

2.4 Weight loss measurement

In the weight loss study, a previously weighed coupon was immersed, with the aid of sewing thread, by suspending it in the blank solution and the solution containing various concentrations (0.25g/L, 0.5g/L, 0.75g/L, 1.00g/L and 1.25g/L) for different interval immersion period (1, 3, 5 and 7hours). The experiments were conducted under total immersion conditions at different temperatures of 298K and 313K and were carried out in triplicates. From the mean results obtained, the percentage inhibitor efficiency (%IE), degree of surface coverage (θ) and the corrosion rate were calculated using equation (1), (2) and (3) [8].

$$\%IE = \frac{(w_0)-(w_1)}{w_0} \text{ X } 100 \qquad (1)$$

Where (W_o) and (W_1) are the weight loss without and with different concentrations of the BALE extracts respectively.

$$\Theta = \frac{(w_o) - (w_1)}{w_o} \quad (2)$$

The expression for measurement of corrosion rate (C_R) in millimeters penetration per year (mm/y) was used to measure corrosion rate (C_R) for the specimens, which was expressed in equation (3) [9].

$$C_R = \frac{86.4\ x\ W}{at\rho} \quad (3)$$

Where, w is corrosion weight loss of mild steel (mg), α is the total surface area of the specimen in (cm^2), t is the exposure time in hours (hr), ρ is the density of the specimen (g/cm^3).

2.5 potentiodynamic polarization measurements

Electrochemical studies were carried out using conventional three electrode cell with larger area platinum foil serving as counter electrode and saturated calomel electrode (SCE) as reference electrode (i.e all measurements were made with reference to this electrode), whereas the mild steel coupons were used as the working electrodes. Autolab Potentiostart (PGSTAT 30 computer controlled) coupled with NOVA software version 1.8 was used for these measurements. The corrosion inhibition efficiency and surface coverage was calculated using equation (4) and (5) [1] [10].

$$IE\ (\%) = \frac{I^0_{corr} - I^i_{corr}}{I^0_{corr}}\ x100 \quad (4)$$

$$\theta = \frac{I^0_{corr} - I^i_{corr}}{I^0_{corr}} \quad (5)$$

Where I^0_{corr} and I^i_{corr} are the corrosion current densities without and with the addition of various concentrations of the inhibitor respectively.

2.6 Surface morphological studies

The surface conditions of the mild steel in contact with 1M HCl acid solutions in the absence and presence of the optimum concentration of the inhibitor were studied with the aid of SEM, UV-visible, XRD and FTIR techniques. The mild steel coupons were retrieved from the solution rinsed with distilled water, dried and then taken for the analysis.

3.0. Results and Discussion

3.1 characterization of Balanites Aegyptiaca Leaves Extract (BALE)

Fig.1 shows FTIR of BALE with the broad peak at 3320 cm^{-1}corresponding to the O-H stretch vibration of alcohols or phenols. The band at 2921cm^{-1} and 2854cm^{-1} with strong peaks correspond to the C-H stretch of alkane usually CH_3, CH_2 or CH, the region at 1722 cm^{-1} shows C=O stretching of acid, the band at 1644 cm^{-1} corresponds to C=O stretching of aldehyde and 1618 cm^{-1} indicates C=C stretch while 1514 $cm^{-1}$and 1208 cm^{-1} are due to N-O asymmetric stretching, C-O-C stretching and 1380 cm^{-1} is due C-H bending respectively. Other peaks include; 1071cm^{-1} and 1045cm^{-1} of C-O 3^o alcohol and 1^o alcohol respectively. 884cm^{-1} and 862cm^{-1} are respectively the bending vibration of C-H deformation. Other bending vibrations include; 754 cm^{-1} C-H aromatic and 672cm^{-1} peak is due to C-H bending vibration also. Thus, results obtained show that BALE contains organic components that are rich in oxygen and aromatic rings, which satisfied the fundamental requirements of a good inhibitor [11].

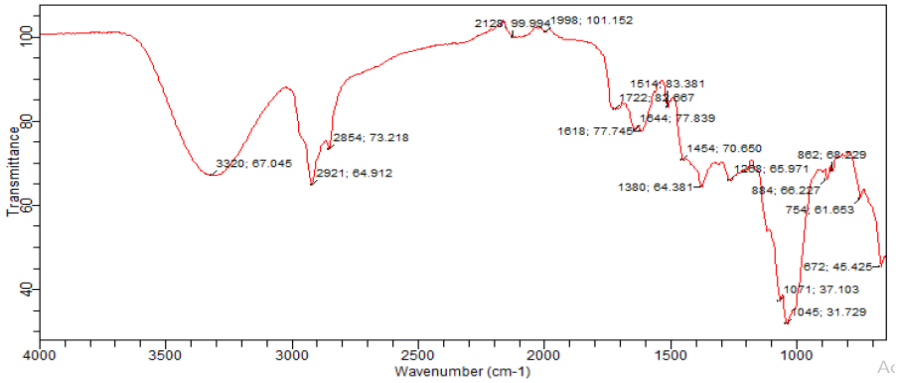

Figure 1: FTIR spectra of as-received Balanites aegyptiaca crude extract.

3.2.0 *Weight loss measurement*

3.2.1 Effect of Immersion Time

Figure 2. Shows the effect of immersion time on the weight loss of mild steel in solutions of 1M HCl in the absence and presence of various concentrations of *Balanites aegyptiaca* leaves extract at 298K. from the plots it can be observed that the weight loss of the mild steel both in the blank and the inhibited solution increase with increasing period of contact but comparatively increased slowly in those obtained for the inhibited solutions and further declined with increase in concentration of the inhibitor indicating that *Balanites aegyptiaca* leaves extract retarded the corrosion reaction of mild steel in the solution of HCl. Similarly, the inhibition efficiencies as seen in figure 3, were found to increase as contact time also increased from 1hr to 7hr showing effectiveness with corresponding increase in concentration of the inhibitor. This can be attributed to the greater degree of the inhibitor molecule being adsorbed on the mild steel surface thereby forming protective layer which inhibited further corrosion attacks by the aggressive media.

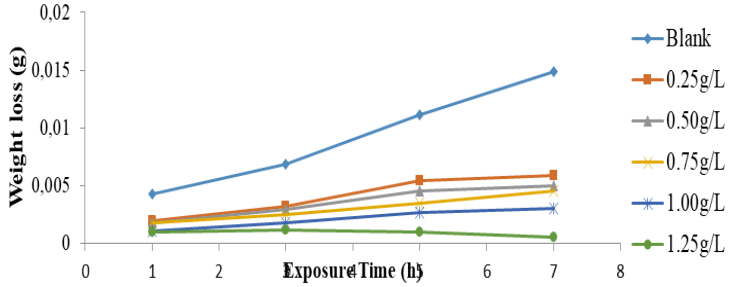

Figure 2: Effect of immersion time on corrosion rate for the corrosion of mild steel in 1 M HCl containing various concentrations of BALE at 298K.

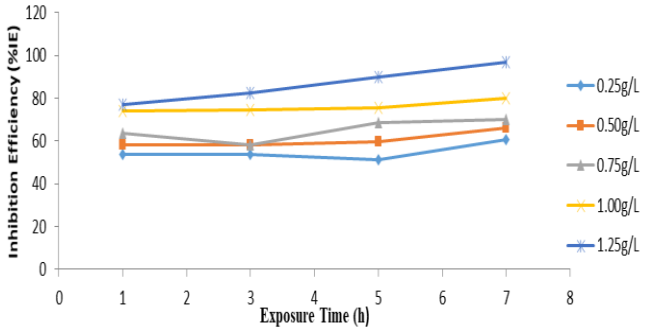

Figure 3: Effect of immersion time on inhibition efficiency for the corrosion of mild steel in 1 M HCl containing various concentrations of BALE at 298K.

3.2.2 Effect of Temperature

The effect of temperature on the inhibition efficiency is shown in figure 4. The results from weight loss study as plotted in Fig 4, revealed that inhibition efficiency of the extract decreases with increasing temperature (i.e from 96.64 % at 298K to 71.91 at 313K in the presence of 1.25g/L concentration as seen in Table 1) which may be attributed to a possible alteration of the adsorption–desorption equilibrium toward desorption of the already adsorbed inhibitor [12]. This decrease in inhibition efficiency with increase in temperature may be also considered as an indication that the inhibitor molecules were not very stable at higher temperature and also that the rate of dissolution of the test metal coupon is readily facilitated at elevated temperature [13].

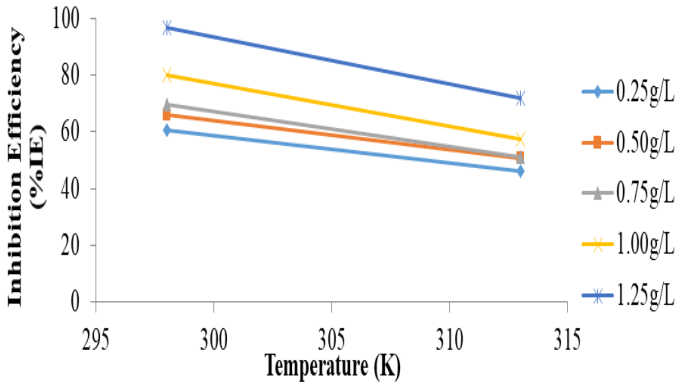

Figure 4: Variation of Percentage inhibition efficiency (%IE) with temperature for mild steel corrosion in 1M HCl in the presence of *Balanites aegyptiaca* leaves extract at various concentrations.

3.2.3 Effect of concentration

Table 1: Inhibition Efficiencies (%IE) and Corrosion Rates for Corrosion of mild steel in the Absence and Presence of Various Concentrations of the studied Extract in 1 M HCl at 298 K and 313 K.

System	**Corrosion rate (mm/y)**		**Inhibition Efficiency (%IE)**	
	298K	313K	298K	313K
Blank	4.29	5.15	-	-
0.25g/L	1.69	2.78	60.40	46.06
0.50 g/L	1.44	2.55	66.08	50.56
0.75 g/L	1.29	2.52	69.79	51.12
1.00 g/L	0.89	2.20	79.87	57.30
1.25 g/L	0.14	1.45	96.64	71.91

Fig. 5 and Table 1 revealed the effect of the concentration of the plant extract on the corrosion rate. It can be observed that there are reductions in the corrosion rate with addition of different concentrations of the inhibitor. As can be seen from Fig. 5 and Table 1, the corrosion rate at Zero (Blank solution) concentration of the inhibitor was found to be considerable as compared with the corrosion rate after addition of various concentration of the inhibitor. Likewise, observed from the figure 6 and Table 1 were increases in the inhibition efficiencies with corresponding increase in the concentrations of the inhibitor molecule. Such behaviors can be due to the appreciable increase of the percentage fractions covered by the

adsorbed active inhibitor phytoconstituents on the mild steel surface and hence, the observed increase in the inhibition efficiency and decrease in corrosion rate [14]

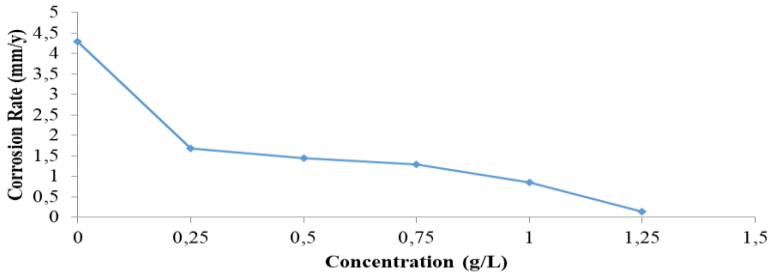

F**igure 5:** Variation of Corrosion Rate of mild steel against Various Concentrations of *Balanites aegyptiaca* leaves Extract in 1 M HCl at 298K.

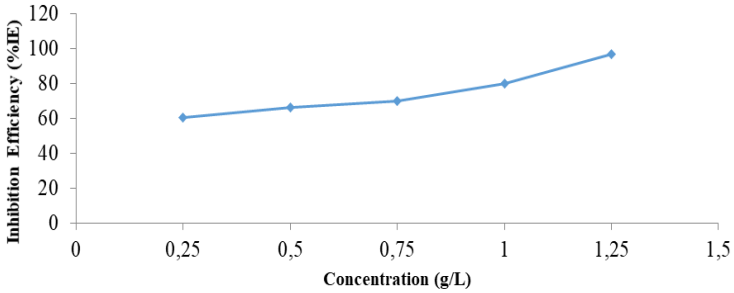

Figure 6: Variation of inhibition efficiency (%IE) against various concentrations of *Balanites aegyptiaca* leaves extract for mild steel corrosion in 1 M HCl solution at 298 K.

3.3.0 Adsorption characteristics

The investigation of the Adsorption characteristics of BALE, steered the present research to the consideration of two adsorption models; Langmuir and Temkin. However, this study found Langmuir isotherm to be the best fit adsorption curve for the extract on mild steel surface in 1M HCl solution showing linearity as indicated in Fig. 7 and Table 2.

3.3.1 Langmuir isotherm

Langmuir adsorption isotherm can be expressed according to the equation (5) [15]. This relates the degree of surface coverage to the concentration of the inhibitor in the bulk electrolyte solution as follows.

$$\frac{C}{\theta} = \frac{1}{K_{ads}} + C \qquad (5)$$

Where C is the concentration of the inhibitor, K is the adsorption equilibrium constant and θ is the degree of surface coverage.

A plot of ($\frac{C}{\theta}$) against C yield linear as shown in Figure 7.

3.3.2. Temkin isotherm

According to Temkin adsorption isotherm, the degree of surface coverage (θ) is related to the inhibitor concentration (C) given by the equation (6) [16].

$$\text{Log}\,\frac{\theta}{C} = \log k_{ads} - g\theta \qquad (6)$$

Where K is the adsorption equilibrium constant and g is the adsorbate interaction parameter. A plot of Log $\frac{\theta}{C}$ against θ as shown in figure gave a linear relationship.

Table 2: Correlation coefficients deduced from Langmuir and Temkin isotherm for mild steel in 1M HCl in the presence of BALE.

Acidic Media	**Langmuir**		**Temkin**	
	R^2	Slope	R^2	Slope
298K	1	1.0263	0.8563	1.5344
313K	0.9973	0.9722	0.8528	1.1453

Langmuir and Temkin isotherms were employed to monitor the interaction between the studied inhibitor molecule and the mild steel surface which usually correlate the surface coverage values, θ to inhibitor concentration, C, in the electrolyte solution. In this study, it can be seen from Table 2, that the Langmuir adsorption isotherms fitted the experimental data as it has a correlation coefficients, R^2 of 1 and a slope of 1.0263 at 298K and R^2 of 0.9973 and slope of 0.9722 at 313K respectively. The R^2 values and slope obtained for Langmuir isotherm are approximately unity, revealing linearity, (indicating that both physical and chemical adsorption processes have taken place) as shown in Fig 7, which showed strong agreement to Langmuir adsorption isotherm model [17]. Consequently, it is evident that the isotherm that best described the adsorption characteristics of *Balanites aegyptiaca* leaves extract onto mild steel surface is Langmuir adsorption isotherm [18] [19].

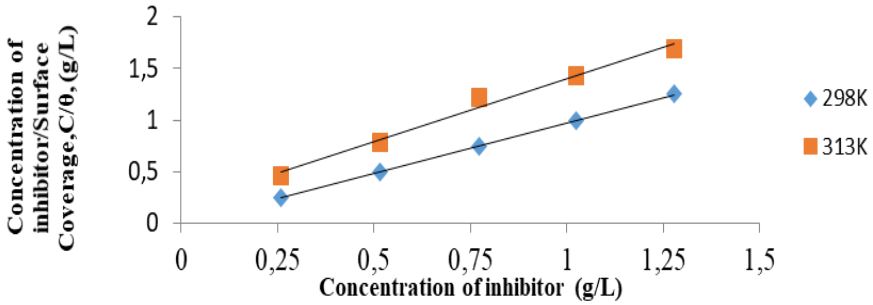

Figure 7: Langmuir isotherm for the adsorption of BALE on mild steel surface in 1M HCl solution.

3.4 Activation Energy

The corrosion rate of mild steel in Hydrochloric acid and the temperatures were related by the Arrhenius equation as shown below [20].

$$C_R = A\exp^{-Ea/RT} \quad (7)$$

$$\log C_R = \log A - \frac{E_{ads}}{2.303RT} \quad (8)$$

$$\log\left(\frac{C_{R2}}{C_{R1}}\right) = \frac{E_{ads}}{2.303R}\left(\frac{1}{T_1} - \frac{1}{T_2}\right) \quad (9)$$

Where C_R = corrosion rate, A= Arrhenius constant, R= Molar gas constant (8.314 J/molK), and T = Kelvin temperature.

The results of activation energies obtained as showed in the Table 3, clearly revealed that the activation energies for the corrosion of mild steel in the presence of BALE increased with increasing concentrations of the plant extracts. The increase of E_{ads} values with concentrations BALE is attributed to significant increase in the degree of adsorption of the inhibitor on metal surface hence, the increase in the reaction rate. In this study, the activation energy, E_{ads} value of 9.45 KJ/mol was obtained in the absence of inhibitor and 25.7 $kJmol^{-1}$ to 121 $KJmol^{-1}$ were obtained for the inhibited systems. This nature of behavior indicated that the inhibitor retarded corrosion at ordinary temperature while the inhibition efficiency is considerably decreased at elevated temperatures [21]. As can be appreciated from Table 3, the E_{ads} values in this research support the proposed physisorption mechanism at lower concentration involving of charge transfer from the inhibitor molecule to Fe in mild steel. But the values at higher concentration are above the threshold value (E_{ads}<80 kJ/mol) required for the mechanism of chemical adsorption [14]. This also supports the suggestion for the adsorption of the inhibitor being comprehensive adsorption [18] [22] [23] [13] [23].

3.5 Thermodynamic Parameters

The free energy of adsorption at different temperatures was calculated from the equation (10) [24].

$$\Delta G_{ads} = -RT \ln (55.5K_{ads}) \quad (10)$$

Where ΔG_{ads} = Gibbs energy of adsorption (J/mole). The constant value 55.5 is the concentration of water in solution in mol/K

The negative values of ΔG_{ads} obtained are attributed with the spontaneity of the adsorption process of the adsorbed layer on the metal surface [25]. Generally the values of ΔG_{ads} up to -20$KJmol^{-1}$ are consistent with electrostatic interaction between charged molecules and a charged metal and the process indicates physical adsorption, while those around −40 KJ mol^{-1} or higher involve charge sharing or transfer from organic molecules to the metal surface to form a coordinate type of metal bond (chemisorption) [25] [14] [23]. In the present study, the values of ΔG_{ads} vary from -21.59 $kJmol^{-1}$ to -33.68$kJmol^{-1}$ at 298K and -19.176 $KJmol^{-1}$ to -20.45 $kJmol^{-1}$ at 313K in 1M HCl for various concentrations revealing that values of ΔG_{ads} at lower temperature are greater than the values required for physical adsorption and are around -40$kJmol^{-1}$, value required for chemical adsorption which indicate that **BALE** functions by not just physically adsorbing onto the metal surface or through a chemical adsorption but following a comprehensive adsorption (physical and chemical adsorption)**.** Similar observations were reported by [23] [13]. Values of ΔG_{ads} were presented in table 3. The heat of adsorption,Q_{ads} was also calculate using the relation below.

$$Q_{ads} = 2.303R \left\{\log\left[\frac{\theta_2}{1-\theta_2}\right] - \log\left[\frac{\theta_1}{1-\theta_1}\right]\right\} X \left(\frac{1}{T_1} - \frac{1}{T_2}\right) \quad (11)$$

Where, θ_1 and θ_2 are degree of surface coverage at temperatures T_1 and T_2 respectively. The calculated values of heat of adsorption Q_{ads} are also given in Table 3. These results revealed that the heats of adsorption were all negative indicating that the adsorption and hence inhibition efficiency decreased with increase in temperature [26]. This also means that there was a spontaneous adsorption of the extract on the metal surface.

The thermodynamic parameters for the enthalpy of adsorption and entropy of the inhibitors on the mild steel (ΔH_{ads}) and (ΔS_{ads}) in the presence and absence of inhibitors was calculated using the transition state equation [27].

$$\frac{C_R}{T} = \frac{R}{Nh} \exp\left(\frac{\Delta Sads}{2{,}303R}\right) \exp\left(\frac{-\Delta Hads}{2{,}303RT}\right) \quad (12)$$

Where N is the Avogadro's Number (6.02252 x 10^{23} mol-1) and h is the Plank's constant (6.626176 x 10^{-34} Js) while other parameters have their usual definition. A plot of $\log\frac{C_R}{T}$ versus 1/*T* gave a straight line with a slope equal to $\left(\frac{-\Delta H_{ads}}{2.303R}\right)$ and an intercept of log $\left(\frac{R}{Nh} + \frac{\Delta S_{ads}}{2.303R}\right)$ from which the values of Δ*S*ads and Δ*H*ads were calculated.

Calculated values of ΔH_{ads} and ΔS_{ads} were also summarized in Table 3. The positive values of ΔH_{ads} mean the endothermic nature of metal dissolution process in the absence and presence of the **BALE** [28] [29]. Also, the increase of ΔH_{ads} with increase in inhibitor concentration revealed that the corrosion rate of the mild steel is largely controlled by kinetic parameters of activation. Physiosorption process is differed from chemisorption as the absolute value of ΔH_{ads} for the physiosorption process is lower than 40 kJ mol^{-1} while that for chemisorption process approaches 100 kJ mol^{-1} [30]. In the present study, some ΔH_{ads} values are less than 40 $kJmol^{-1}$ which fits the description for common physical adsorption enthalpy at lower concentration, but some values are found to be greater than the threshold for chemical adsorption enthalpy (100 kJ mol^{-1}) at higher concentration, this phenomenon also led to the conclusion that both physical and chemical adsorption took place. [18] [23] [30] reported similar explanations. The fact that all values of ΔS_{ads} are negative, this behavior can be explained in that the inhibitor molecules before adsorption on to the metal surface, might had been chaotically moving freely in the bulk solution but as the adsorption process advanced, the inhibitor molecule were orderly adsorbed on to metal surface, consequently a decrease in entropy is observed [23] [31] [32].

Table 3: Thermodynamic and kinetic parameters calculated from weight loss measurements studies

Concentration (g/L)	E_a ($KJmol^{-1}$)	Q_{ads} ($KJmol^{-1}$)	ΔG_{ads} (KJ/mol) 298K	ΔG_{ads} (KJ/mol) 313k	ΔH_{ads} ($KJmol^{-1}$)	ΔS_{ads} ($Jmol^{-1}$)
Blank	9.45	—	—	—	7.0	-210
0.25	25.7	-1.11	-21.59	-19.18	23	-151
0.50	29.6	-1.80	-20.49	-19.14	27	-163
0.75	34.6	-2.26	-20.52	-18.84	32	-135
1.00	48.6	-3.72	-24.88	-18.74	46	-92.0
1.25	121	-9.06	-33.68	-20.45	118	-40.1

3.6 Potentiodynamics polarization techniques

The polarization curves obtained for mild steel in 1M HCl solution with and without various concentrations of *Balanites aegyptiaca* leaves extract at 298K are presented in Figure 8.From the results in Table 4, it is observed that the I_{corr} values gradually decreased with corresponding increases in the concentration of the inhibitor till 1.25g/L (1.142 $mAcm^{-2}$ to 7.5x 10^{-7} $mAcm^{-2}$) yielding 99.99% of Inhibition Efficiency at the optimum concentration of 1.25g/L showing that the anodic reaction was affected and therefore, retarded. On the other hand, there was a cathodic shift of the E_{corr} values towards more negative value signifying that the cathodic reaction was also inhibited by the presence of the inhibitor molecules. These changes in both anodic current density and the cathodic corrosion potentials showed that the BALE functioned as an anodic-cathodic type inhibitor in 1M HCl solution. These deductions can further be supported by taking observing the gradual and significant decrease in both Tafel slopes constants (Branches) towards lower current densities as can be seen from Fig. 8 and Table 4. Consequently, it could be deduced from these observations that the rates of anodic dissolution as well as cathodic hydrogen evolution were practically retarded. This means that the extract must have acted as mixed-type of the 1M HCl acid corrosion inhibitor. Similar behaviors have been reported in the works of other researchers as [18] [22] [33] [34] [35].

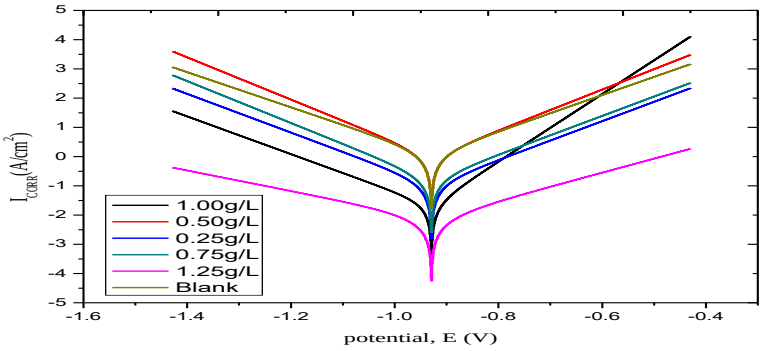

Figure 8: Tafel polarization curve from potentiodynamic polarization measurements

Table 4: Electrochemical parameters, inhibition efficiency and surface coverage obtained from potentiodynamic polarization studies

Conc. of inhibitor(g/L)	Ba (mV/de)	βc (mV/de)	E_{CORR} (mV)	I_{CORR} (mA/cm^2)	Corrosion Rate Cr(mm/y)	Polarization resistance Rc (Ω)	Surface coverage	IE (%)
Blank	160.80	166.34	-854.96	1.142	13.265	31.105	—	—
0.25	150.87	151.12	-915.85	1.070	12.431	30.651	0.0631	6.300
0.50	145.95	140.99	-778.04	0.895	10.398	34.803	0.2163	22.00
0.75	133.42	53.633	-891.70	0.079	0.9179	210.31	0.9308	93.00
1.00	8.6560	15.499	-929.68	2.2E-3	0.0252	1113.2	0.9981	99.80
1.25	2088.8	285.49	-1036.7	7.5E-7	8.72E-6	6.98E7	0.9999	99.99

3.7. *FTIR Spectrophotometric Analysis*

Figures 9a and 9b represent the IR spectra of *Balanites aegyptiaca* leaves extract (crude) and that of the corrosion product on mild steel. It was found that C=O stretch at 1644 cm^{-1}, 2128 cm^{-1} due to -C=C-, 1208 cm^{-1} due to C-O-C, 1722 due to C=O were all disappeared. However, shifts were also observed from 1208 cm^{-1} to 1205 cm^{-1} and from 1618 cm^{-1} to 1611 cm^{-1}, also, from 1076 cm^{-1} to 1086 cm^{-1} assigned to C-O, likewise, 2128 cm^{-1} shifted to 2117 cm^{-1} due π −bond in –C=C- and appearance of 1016 cm^{-1}, 1676 cm^{-1}, 1834 cm^{-1}, 3905 cm^{-1} etc as can be seen from Figures 4.12a and 4.12b indicating that there are strong both physical and chemical interaction between the inhibitor molecules and mild steel surface. The bands at 1016 cm^{-1} to 1834 cm^{-1} and 3589 cm^{-1} to 3905 cm^{-1} presumably originate mainly from β-Fe_2O_3 which may be due to chemical mechanism adsorption. Other functional groups were missing and some appeared as stated above suggesting

that the adsorption of the inhibitor on the surface of mild steel might have occurred through the missing bands and the appearance of new ones [11].

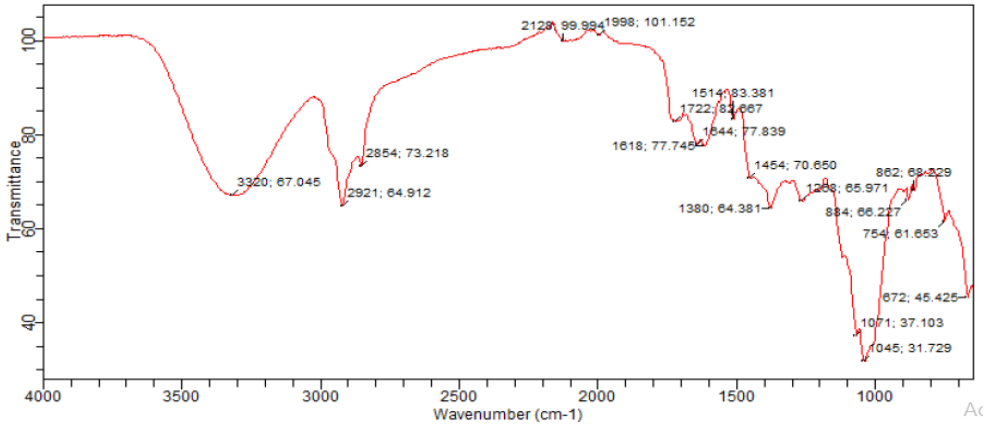

Figure 9a: FTIR spectra of as-received BALE.

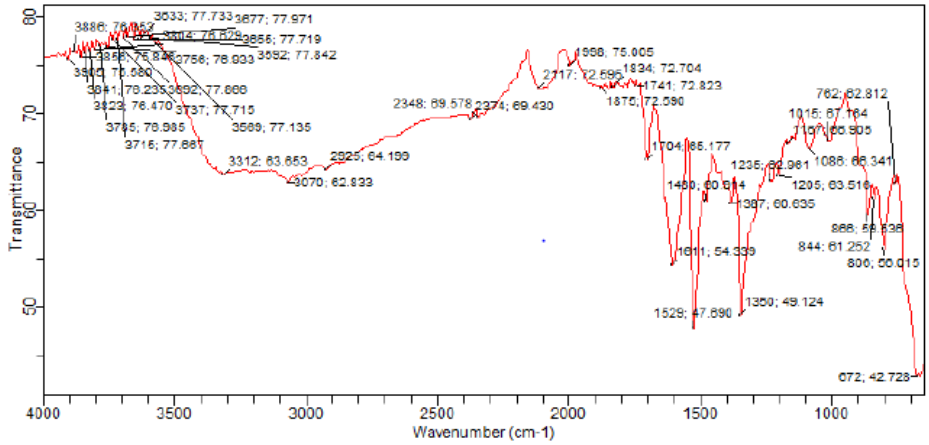

Figure 9b: FTIR spectra of as-received corrodent solution after immersion tests.

3.8 UV-Visible Spectroscopy Analysis

The observed variation in the absorbance (spectra) before and after immersion of mild steel as shown in Fig 10a and 10b, can be used to confirm the possibility of the formation of BALE-Fe complex. This complex formation may be responsible for the observed deviation in the absorbance and its intensity value and also may be responsible for anticorrosion activity. Also, the study of the absorbance spectra for the pure *Balanites aegyptiaca* leaves extract, the shift and significant alteration (i.e shift of band from 227.84nm to 223.84nm and appearance of new bands like 203.94nm, 207.99nm and 325nm) in the shape of the corrosion products spectra, is an indication that both physical (only shift in the peaks value) and chemical (appearance of new peaks) adsorptions might have occurred. This demonstration of strong interactions is favorable suggestion for the formation of thin inhibitor layer over the mild steel surface [36]. In conclusion, the wide variation existing between the two spectra offered a plausible evidence to support the prediction made about the occurrence of comprehensive adsorption (physical and chemical adsorption) in this study [18] [22] [13] [23] [30] [37] [38].

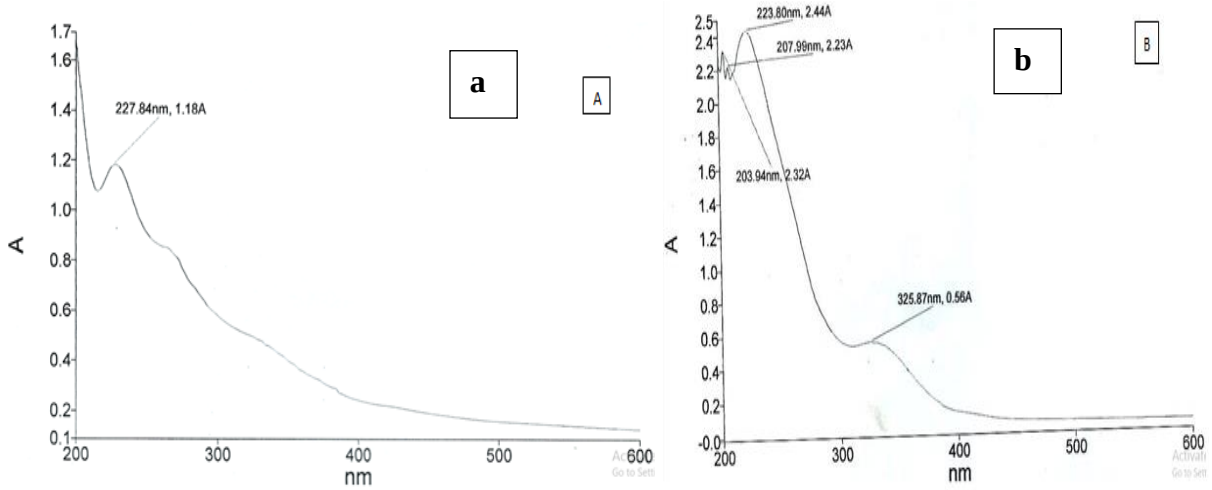

Figure 10: UV-Visible spectrum of (a) corrosion products solution of mild steel immersed 1M HCl containing 1.25g/L BALE (b) UV-Visible spectrum of pure BALE.

3.9. Mechanism of Inhibition

The present evaluation considered two possible modes of adsorption from examination of FTIR and UV-Visible pattern:

(1) Chemosorption mechanism: In this mode, there will be an attempt by the neutral BALE to adsorb onto the mild steel by forming covalent bonds with the metal surface through sharing of electrons (lone pair electron) from the oxygen atoms to the appropriate vacant d-orbital of the iron. Interaction between the pi-bond or sigma bonds on the aromatic ring and vacant 3d-orbital can also occur via adsorption in the donor-acceptor type of bond. Physiosorption mechanism: there is propensity that BALE would get protonated given its environment which consist of extra H^+ from HCl, subsequently, the protonated inhibitor molecule in BALE may adsorb on the metal surface creating electrostatic interactions between the positively charged molecules and the negatively charged metal sites, (i.e cathodic area). In other words, there may be an interaction between Cl- and BALE, which enhances the inhibitive potential of the inhibitor. There may be also the formation of a coordinate bond by partial electrons transfer from the polar atoms (O atoms) to the metal surface, when the protonated BALE is adsorbed on the metal surface. Furthermore, given the lone-pair electrons nature of O atom in BALE or protonated BALE may combine with oxidized Fe^{2+} ions on steel surface forming metal inhibitor complexes:

$$Fe \longrightarrow Fe^{2+} + 2e^- \quad (13)$$

$$BALE + Fe^{2+} \longleftrightarrow [DVLE\text{-}Fe]^{2+} \quad (14)$$

$$[BALEH_y]^y + Fe^{2+} \longleftrightarrow [BALEH_y\text{—}Fe]^{(2+y)+} \quad (15)$$

Mechanism of similar type was also proposed by [11] [39]. These complexes might be adsorbed onto steel surface by vander Waals force to form a protective film to prevent mild steel from corrosion. The main constituents of the extract are diosgenyl Saponins: balanitin-7[40]

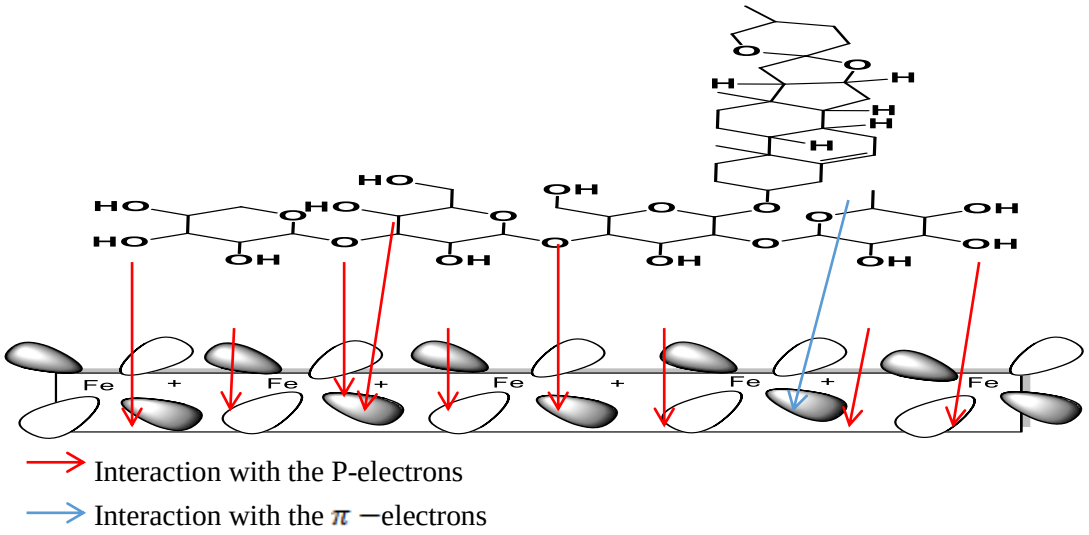

Figure 11: Depiction of interaction mechanism between active sites of balanitin-7 and mild steel surface [41] [42].

3.10. Scanning Electron Microscopy (SEM) Analysis

The SEM micrograph image in Fig. 12a showed that the mild steel specimen immersed in inhibited solution suffered minimal if any visible damages and it has a fairly smooth surface. This provided proof of corrosion inhibition effectiveness of *Balanites aegyptiaca* leave extract against the mild steel corrosion in 1M HCl solution. In order words, it has far better surface condition. Similarly, presented, in Fig 12b, is a SEM micrograph of the mild steel surface immersed in the uninhibited 1M HCl solution. Unlike the micrograph image in Fig. 12a, the micrograph image in Fig. 12b as can be seen possesses a very rough surface full of numerous corrosion crevices and products and in addition to those, also consists of many pits and corrosion cavities from the corrosion attacks. These experimental results showed strong evidence for formation of a barrier thin layer by the inhibitor molecule which effectively protected the mild steel surface against the corrosion reaction. Similar research findings have been reported by many researchers [18] [1] [43] [44].

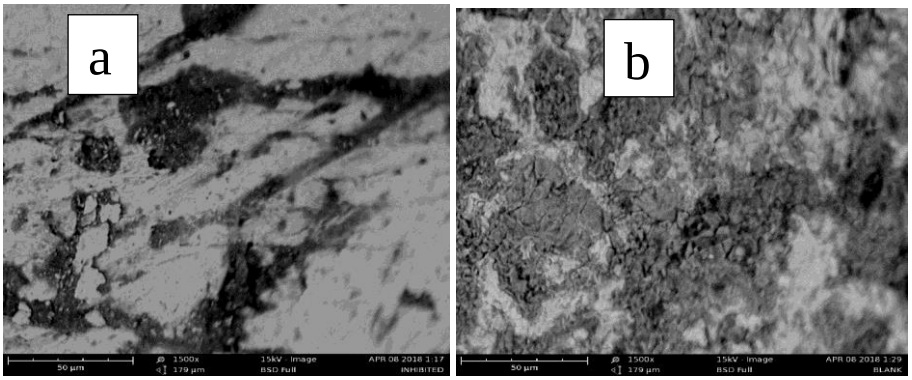

Figure 12: SEM micrograph of (a) mild steel immersed in 1M HCl solution (b) mild steel immersed in 1M HCl containing 1.25g/L of BALE for 7 hours.

3.10 X-ray Diffraction Pattern Analysis

The XRD patterns of the mild steel in the presence and absence of the inhibitor in 1M HCl is presented Fig. 13a and 13b. The relative peak intensities of the patterns are well consistent with the Solid Diffraction File distributed by the International Centre for Diffraction Data (ICDD). Figures 13a and 13b showed the XRD patterns of the mild steel surface in 1 M HCl acid solution and the mild steel surface immersed inhibited acid solution containing 1.25g/L for 7

hours. The diffraction pattern in Fig 13a has peaks at angle 37.1° and 57° which were characteristics of goethite and $FeCl_2$ showing rough surface while those at 46.1° and 66.5° are those of Fe respectively. But in the Fig 13b there are peaks at 50.2°, 40.8° and 30.1° with no characteristic appearance of $FeCl_2$ with a fairly smoother surface when compared to Fig. 13a. These patterns revealed the non-crystalline nature of the surface which is presumed to be those of the iron-inhibitor complexes layer. The study of the XRD patterns of the mild steel surface in 1M HCl acid solution and the mild steel surface immersed in the inhibited acid solution containing 1.25g/L clearly revealed the formation of adsorbed layer. This information from XRD patterns provided evidence that there was an adhered interaction between the mild steel surface and the studied inhibitor molecules that formed thin protective layer which inhibited the corrosion attack on the metal surface. This confirmed the complexing processes [45] [46].

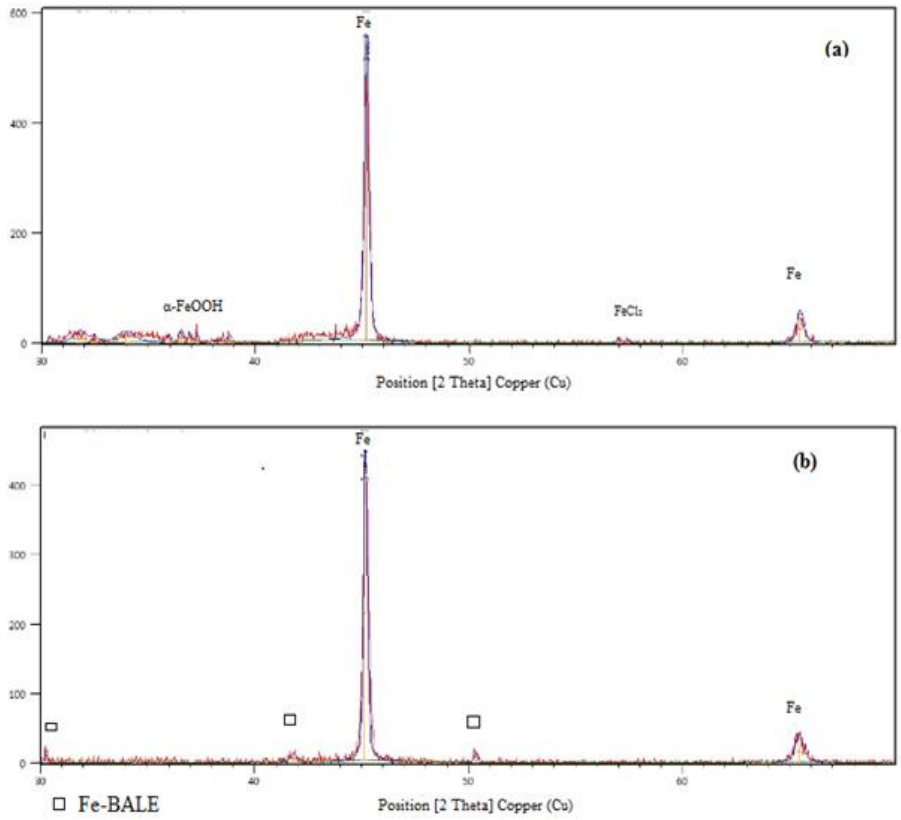

Figure 13: XRD pattern of mild steel surface (a) after immersion in 1 M HCl solution (b) after immersion in the inhibited solution containing 1.25g/L of BALE for 5 hours.

4.0 Conclusions

- This study shows that the **BALE** as corrosion inhibitors have better efficiency towards corrosion inhibition of mild steel which increase with increase in the concentration of inhibitor and decreases with rise in temperature.
- The positive value of ΔH_{ads} and negative value of ΔS_{ads} indicates endothermic reaction which proceeds with decreases in randomness at the solid-liquid interface and ΔG_{ads} values indicates the spontaneous adsorption of the inhibitor.
- Also thermodynamics parameters in this study suggested the inhibition adsorption mechanism as comprehensive adsorption.
- The adsorption of the inhibitor best follows Langmuir adsorption isotherm.

- FT-IR, UV-visible and XRD indicate that there is complexation process between the inhibitor molecules and iron ions which formed protective layer on the mild steel surface.
- SEM confirmed the anticorrosion action of BALE on mild steel in 1 M HCl solution.
- Potentiodynamic polarization curves indicate that the inhibitor behaves as mixed type inhibitor.

References

[1] A. Salhi, A. Bouyanzer, A. Chetouani, S. El Barkany, H. Amhamdi, I. Hamdani, A. Zarrouk, B. Hammouti, J.M. Desjobert and J. Costa, Mor. J. Chem. 5 N°1 (2017) 59-71

[2] K. K. Anupama, K. Ramya, and A. Joseph, Journal Molecular Liquids, 216 (2016) 146-155.

[3] N. Lebe, N. George, E. N. Justus, and E. Peter, International Journal of Materials and Chemistry 6 (2016) 12-18.

[4] C. A. Loto, T. R. Loto, and .I. P. A Popoola, International Journal of Physical Sciences, 6 (2011, August 4) 3616-3623.

[5] L. C. Daya. and H. U. Vaghasiya, Pharmacognosy Revivew.5 (2011) 55-62.

[6] J. B. Hall, Forest Ecological Management. 50 (1992) 1-30.

[7] C. N. Pandey, Medicinal plants of Gujarat; Gujarat, India: 1 (2005) 387-398.

[8] K. F. Khaled, International Journal of Plant, Animal and Environment, 3 (2008) 462-475.

[9] S. M. Adams, S. A. Yaro, M. Abdulwahab, and E. E. Oguzie, Nigerian Journal of Technology (NIJOTECH), 35, No. 4 (2016). 888 – 894.

[10] B., Usman, H. H. Abdallah, H. Maarof, and M. Aziz, Bayero Journal of Pure and Applied Sciences, 10 (2015) 590 – 595.

[11] S. Leelavathi,. and R. Rajalakshmi, Journal of Material and Environmental Science. 4 (2013) 625-638.

[12] H. Derfouf, Y. Harek, and L. Larabi, International Journal of Environmental Engineering.Volume 1 (2014) 234-249.

[13] H. Zarrok, H. Oudda, A. Zarrouk, R. Salghi, B. Hammouti and M. Bouachrine, Der Pharma Chemica, 3 (2011) 576-590

[14] N. O. Eddy, U. J. Ibok, E. E. Ebenso, A. El-Nemr, and H. E. El Sayed, Journal Of Molecular Model. 15 (2009) 1085–1092

[15] S. Bilgic, and M. Sahin, Material Chemistry and Physics.70 (2001) 290-295.

[16] S. S. Fernando, G. Cristiano, S. G. Reinaldo, and S. Almir, Materials Science and Engineering.3 (2012) 2436–2444.

[17] S. Acharya, and S. N. Upadhyay, Transaction of the Indian Institute of Metal. 57 (2004) 297-306.

[18] B. K. Subrahmanya, H. Lgaz, R. Salghi, A. Chaouiki, Shubhalaxmi, and S. Jodeh, Cogent Engineering (Material Engineering and Research Article) 5 (2018) 1-17. 1441585. https://doi.org/10.1080/23311916.2018.1441585

[19] D. Magaji, P. O. Ameh, N. O. Eddy, A. Uzairu, A. A. Siaka, S. Habib, M. A. Ayuba, and S. M. Gumel, Interenational Journal of Modern Chemistry. 2 (2012) 64-73.

[20] H. F. Chahul, A. M. Ayuba, and S. Nyior, ChemSearch Journal 6 (2015) 20–30. Publication of Chemical Society of Nigeria, Kano Chapter.

[21] S. S. Abd El Rehim, S. Refaey, F. Taha, M. B. Saleh, and R. A. Ahmed, Journal of Applied Electrochemistry, 31 (2001) 429-435.

[22] H. Lgaz, R. Salghi, S. Jodeh, and B. Hammouti, Journal of Molecular Liquids, 225 (2107) 271–280. doi:10.1016/j.molliq.2017.11.039.

[23] E. A. Noor, and H. A. Aisha, Materials Chemistry and Physics, 110 (2008)145-154

[24] Q. B. Zhang, and Y. X. Hua, Electrochimica Acta, 54 (2009) 1881-1887
[25] F. Bentiss, M. Lebrini, M. Lagrenee, Corrosion Science, 47 (2005) 2915-2931.
[26] H. M. Bhajiwala, and R.T. Vashi, Bulletin of Electrochemistry. 17 (2001) 441- 446.
[27] S. Ambrish, V. K. Singh, and M. A. Quraishi, Journal of chemistry. 3 (2010) 811-824.
[28] A. S. Umoren, The Open Corrosion Journal, 2 (2009) 175-188.
[29] M. A. Quraishi, A. Singh, V. K. Singh, D. K. Yadav, and A. K. Singh, Materials Chemistry and Physics, 122 (2010) 114–122.
[30] M. Benabdellah, R. Touzani, A. Dafali, M. Hammouti, S. El Kadiri, Material Letter. 61 N^0 4-5, (2007) 1197-1204
[31] K. Nurul Izni, and J. Kassim, International Journal of Electrochemical Science. 8 (2013) 7138-7155
[32] X. Li, S. Deng, H. Fu, and T. Li, Electrochimica Acta, 54 (2009) 4089-4098.
[33] Z. Salarvand, M. Amirnasr, M. Talebian, K. Raeissi, and S. Meghdadi, Corrosion Science, 114 (2017) 133–145. https://doi.org/10.1016/j.corsci.2016.11.002.
[34] J. Huang, H. Cang, Q. Liu, and J. Shao, International Journal of Electrochemical Science, 8 (2013) 8592–8602.
[35] W. H. Li, Q. He, S. T. Zhang, C. L. Pei, and B. R. Hou, Journal of Applied Electrochemistry, 38 (2008) 289–295.
[36] J. R. Premjith, D. K. J. Vishnu, S. Ramkumar, and P. M. Keerthy, International Journal of Corrosion. 1 (2014) 1-6. Article ID; 487103. http//dx.doi.org/10.1155/2014/487103.
[37] X. Li, and G. Mu, Applied Surface Science. 252 (2005) 1254-1265.
[38] L. Tang, G. Mu, and G. Liu, Corrosion Science 45 (2003) 2245-2251.
[39] Xianghong, Li, D. Shuduan, F. Hui, Corrosion Science. 62 (2012) 163-175.
[40] T. Azene, International Journal of Modern Chemistry and Applied Science. 2 (2015), 189-194.
[41] F. Gapsari, R. Soenoko, A. Suprapto, and W. Suprapto, International Journal of Corrosion. 2015(2015) 1-10. Article ID 567202, http://dx.doi.org/10.1155/2015/567202.
[42] G. Chen, M. Zhang, J. Zhao, R. Zhou, Z. Meng, and J. Zhang, Chemistry Central Journal,. 7 (2013) 345-351.
[43] M. H. Mahross, K. Efil, T. A. S. El-Nasr, and O. A. Abbas, Journal of Electrochemical Science and Technology, 8 (2017) 222-235.
[44] I. Ahamad, R. Prasad, M. A. Quraishi, 2010. Adsorption and Inhibitive Properties of some Mannich Bases of Isatin Derivatives on Corrosion of Mild Steel in Acidic Media Corrosion Science., 52 (2010) 3033-3441.
[45] M. Cabrini, S. Lorenzi and T. Pastore, International Journal of Corrosion. 2016 (2016) 1-7 Article ID 3121247, http://dx.doi.org/10.1155/2016/3121247.
[46] A. Hamdy, and N. S. El-Gendy, Egyptian Journal of Petroleum, 22 (2013) 17–25.